Excitonic resonances in thin films of WSe 2 : from monolayer to bulk material

Ashish Arora, Maciej Koperski, Karol Nogajewski, Jacques Marcus, Clement Faugeras, Marek Potemski

Excitonic resonances in thin films of WSe_2: From monolayer to bulk material

Ashish Arora,*,† Maciej Koperski,† Karol Nogajewski,† Jacques Marcus,‡ Clément Faugeras,† and Marek Potemski*,†

Laboratoire National des Champs Magnétiques Intenses CNRS-UJF-UPS-INSA, 25 rue des Martyrs, 38042 Grenoble, France, and Institut Néel, CNRS-UJF, BP 166, 38042, Grenoble, France

E-mail: ashish.arora@lncmi.cnrs.fr; marek.potemski@lncmi.cnrs.fr

Abstract

We present optical spectroscopy (photoluminescence and reflectance) studies of thin layers of the transition metal dichalcogenide WSe_2, with thickness ranging from mono- to tetra-layer and in the bulk limit. The investigated spectra show the evolution of excitonic resonances as a function of layer thickness, due to changes in the band structure and, importantly, due to modifications of the strength of Coulomb interaction as well. The observed temperature-activated energy shift and broadening of the fundamental direct exciton are well accounted for by standard formalisms used for conventional semiconductors. A large increase of the photoluminescence yield with temperature is observed in WSe_2 monolayer, indicating the existence of competing radiative channels. The observation of absorption-type resonances due to both neutral and charged excitons in WSe_2 monolayer is reported and the effect of the transfer of oscillator strength from charged to neutral exciton upon increase of temperature is demonstrated.

*To whom correspondence should be addressed

†Laboratoire National des Champs Magnétiques Intenses CNRS-UJF-UPS-INSA, 25 rue des Martyrs, 38042 Grenoble, France

‡Institut Néel, CNRS-UJF, BP 166, 38042, Grenoble, France

Introduction

Atomically thin layers of semiconducting transition metal dichalcogenides (SC-TMDCs) of the form MX_2 (such as MoS_2, $MoSe_2$, WS_2 and WSe_2) attract a considerable research interest stimulated by the scientific curiosity to study a new class of two-dimensional (2D) semiconductors and by their potential applications in optoelectronics, photonics and the development of valleytronics.[1–7] Bulk MX_2 crystals, largely investigated in the past,[8–10] consist of weakly bonded X-M-X monolayer units (three atomic planes). Monolayer (1 ML) and few-, N-monolayer (N ML) flakes of SC-TMDCs can be conveniently extracted from bulk crystals and deposited on substrates using the methods of mechanical exfoliation.[11] Since very first works on MoS_2 layers,[1] it is now well established that the band structure of N MLs of SC-TMDCs critically depends on N. Monolayers of SC-TMDCs are believed to be direct band gap (or nearly direct band gap) semiconductors and undergo a crossover to the indirect band gap structure of bulk SC-TMDCs with increasing N.[12–14] Strong excitonic (Coulomb) effects, whose strength may also vary with N, is another relevant ingredient which determines the optical properties of thin films of SC-TMDCs.[14] A thorough understanding of basic optical properties of these films is essential for advancing their further explorations, towards efficient future applications.

In this paper, we report on optical investigations of thin films of WSe_2 with thicknesses ranging from 1 ML to 4 ML and bulk flakes, using micro-photoluminescence (μPL), micro-photoluminescence excitation (μPLE) and micro-reflectivity contrast (μRC) spectroscopy techniques, in 5 K-300 K temperature range. Our N-layer WSe_2 structures are first characterized with low temperature, band-edge μPL and absorption-type experiments which depict the characteristic indirect to (nearly) direct band gap crossover, when approaching from thicker to the 1 ML film. We then focus on the evolution of absorption resonances as a function of N in a broader energy range, as they are derived from μRC measurements. The ground state A and spin-orbit (SO) split B excitons associated with the K-point of the Brillouin zone are each accompanied by the excited state resonances A^* and B^*, respectively. Energy separation between A and A^*, and between B and B^* varies with N, which reflects the changes in the strength of excitonic binding as well as in the character of excitonic states, from non-Rydberg states in 1 ML to rather Rydberg like states in bulk. Another clear absorption resonance C, observed in the upper spectral energy range and most sensitive to N, is tentatively assigned to the transition at the M-point of the Brillouin zone. Energy shift and broadening of the ground state A exciton resonance with increasing temperature are both well accounted for by conventional formulae for the band gap shrinkage and optical phonon mediated broadening of free exciton emission, which have been widely applied to other semiconductors. Strikingly, the integrated PL intensity in the 1 ML of WSe_2 is found to increase considerably with temperature, whereas opposite is observed in conventional direct band gap semiconductors. Although neutral excitons (which dominate the PL spectra at high temperature) have higher emission efficiency than the bound/charged excitons (which dominate the PL at low temperatures),[15,16] this observation of an enhancement of integrated intensity is a thinkable sign of the presence of a radiatively inefficient channel at low temperature, which upon thermalization, transfers the carriers to radiatively efficient channel at higher temperatures. It opens up scope for further investigations and discussions on this material. Finally, both neutral (A) and charged (trion, T)[17–20] excitonic resonances are observed in 1 ML flake not only in emission, but in absorption-type μRC spectra as well. This allows us to demonstrate the effect of transfer of oscillator strength from trion to exciton, upon increasing the temperature.[21–24] Further studies of the effects of the presence of free carriers on the optical response of the WSe_2 monolayers are highly desirable.

Samples and characterization

For preliminary characterization of the flakes, we performed atomic force microscopy (AFM) and μPL measurements on the flakes. Insets to the Fig. 1 (c-e) show the optical images of the flakes. The thicknesses of the 1 ML, 2 ML, 3 ML, 4 ML as well as the bulk flake were found to be $\sim$0.7 nm, $\sim$1.4 nm, $\sim$2.1 nm, $\sim$2.8 nm and $\sim$20 nm respectively using AFM (data not shown). The PL spectra of the flakes have been shown as solid curves in Fig. 1(a-e). The 1 ML thick flake is found to emit light most efficiently, and the emission intensity reduces considerably as the thickness of the flakes is increased. A reduction in intensity by 4 orders of magnitude is observed when the flake thickness is increased from 1 ML to 20 nm. It is because the nature of the band gap changes from direct to indirect for thickness greater than 1 ML.[13] The emission also shifts to lower energy with increasing flake thickness. This indicates the reduction of the fundamental bandgap with an increased flake thickness, in analogy to the effect of quantum confinement in semiconductor quantum wells.

To gain more insight into the near band-edge properties of our layers, apart from μPL, we performed μPLE and μRC spectroscopy studies on the same flakes. The well pronounced, lowest energy absorption resonance seen in these spectra (dashed blue and dashed red traces in Fig. 1) is identified with the so-called A exciton associated to the direct band alignment of WSe_2 at K-point of the Brillouin zone. Its double peak structure in the monolayer (trion T resonance on the low energy side) and in the bulk sample (excited exciton state A^* on the higher energy side) will be discussed later on. A small shift in the absorption resonances seen in the PLE spectra and

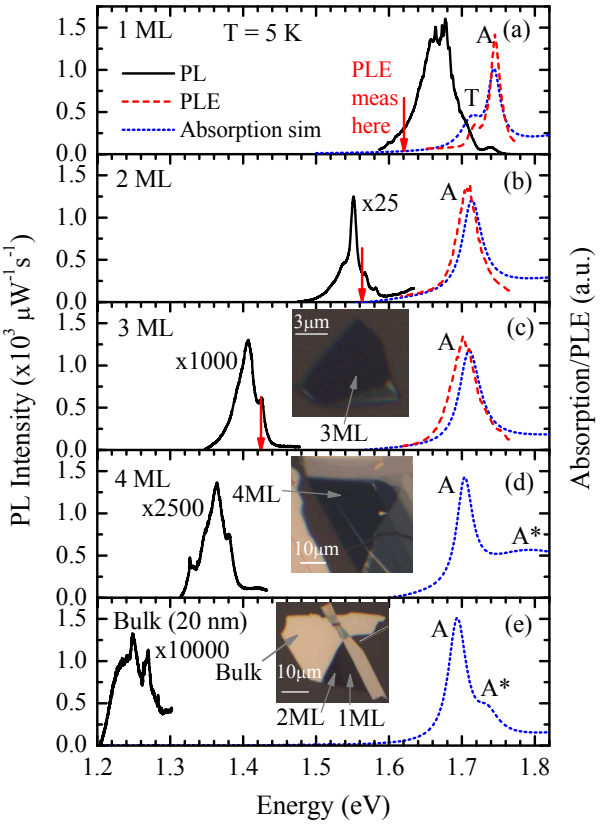

Figure 1: Solid lines in (a-e) show the PL spectra for a 1 ML, 2 ML, 3 ML, 4 ML and 20 nm thick flakes respectively. Dashed red lines in (a-c) are the PLE spectra of the corresponding flakes, obtained by monitoring the PL emission intensity at an energy shown by the arrows. The dotted curves are the absorption spectra simulated from the modeling of the reflectance contrast spectra of the corresponding flakes. The insets to (c) and (d) show the optical image of a 3 ML and 4 ML thick flakes whereas the inset to (e) shows a flake which contains 1 ML, 2 ML and 20 nm thick bulk flakes used for the study.

those extracted from μRC measurements is likely due to effectively higher sample temperature in the course of PLE measurements which imply the use of laser excitation and unavoidable local heating effects, and/or due to energy sensitive carrier relaxation process which may also alter the shape of absorption as reflected in PLE spectra.

One of the prominent and clear features of the data shown in Fig. 1 is the red shift of the PL spectra with respect to the fundamental absorption resonances. This shift progressively increases with the number of layers. It is pretty large ($\sim$150 meV) for the WSe_2 bilayer and up to $\sim$500 meV in the bulk sample. The logic of indirect and low energy transitions giving rise to the PL spectra but direct and higher energy transitions determining the absorption resonances is consistent with the indirect fundamental band gap in all WSe_2 layers with N$\geq$2. Instead, however, the monolayer WSe_2 is believed to be a direct band gap semiconductor. Its strong emission intensity and partially overlapping emission and absorption spectra (practically common emission and absorption peak due to A exciton) are in favor of this scenario. The main part of the low temperature emission spectrum of WSe_2 monolayer appears still below the fundamental absorption resonance, what is, however, commonly attributed to the recombination process due to localized/bound and/or charged excitonic complexes.

Absorption resonances versus layer thickness

In Fig. 2(a), we present the results of RC experiments performed at T = 5 K for the same flakes in a wide range of energy (spectra are shifted vertically for clarity). Three dominant resonances, labelled A, B and C are observed for all the different flakes. A and B are attributed to the two ground state ($n = 1$) excitonic absorptions at the K-point of the Brillouin zone while the origin of the excitonic absorption C (labeled as A$'$ in some works following Ref. 8) is still a matter of debate.[8,13,25–27] Recent **k**·**p** calculations predict van-Hove singularities at both K and M points, with a transition energy $\sim$3 eV for 1 ML.[27] Considering an excitonic binding energy equal to that of A-exciton (0.37 eV)[28] as a first approximation, then the exciton transition energy of $\sim$2.6 eV agrees with our observation of C-exciton. Another report predicted theoretically that the possible transition at M-point should red shift by $\sim$100 meV when the flake thickness is increased from 2 ML to bulk.[30] This is in qualitative agreement with our observed red shift of $\sim$140 meV in C-exciton indicating that this feature possibly originates from the M-point of the Brillouin zone. In addition, the behaviour of C-exciton is in contrast with that shown by the A-exciton transition where the ob-

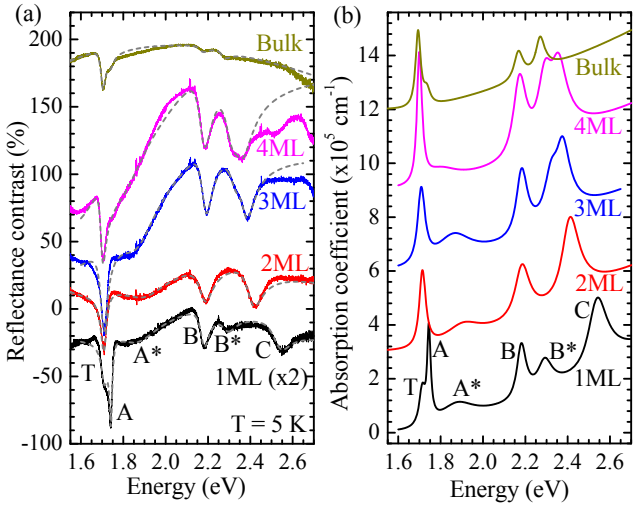

Figure 2: (a) represents the reflectance contrast spectra of the flakes shown in Fig. 1 with sample kept at 5 K temperature. The dashed lines are the lineshape fits to the corresponding spectra. (b) shows the absorption coefficient of the flakes derived from the lineshape fittings. In both the plots, the spectra for the layers with thickness $\geq$2 ML have been shifted along the **y**-axis for clarity.

served shift is only a $\sim$20 meV, and the former is therefore unlikely to have the much debated similar origins as A-exciton i.e. at the K-point. In all the flakes, A and B excitons are accompanied by a broad shoulder at high energy side of the excitons. We associate these features with the contributions due to the excited state (n = 2 and onwards) A* and B* exciton transitions. This is in accordance with a recent study where the excited states of A exciton in WSe_2 MLs were observed at an energy range lying $\sim$160 meV to $\sim$370 meV above the A resonance.[28] A collective contribution of all these states gives rise to a rather broad feature in RC spectra. Furthermore, in the case of 1 ML thick flake, a feature appears towards lower energy side of the A-exciton. As discussed later, we identify this shoulder as the spectral contribution due to the formation of the trion T (cherged exciton). Additional high energy features appear in the RC spectra of the flakes thicker than 2 ML. An assignment of these features requires a more detailed theoretical and experimental work.

For the lineshape analysis of the RC spectra, we followed a method similar to that described in Ref. 31. In this method, we considered the excitonic contribution to the dielectric response function to be given by a Lorentz oscillator like model as

$$\varepsilon(E) = (n_b + ik_b)^2 + \sum_p \frac{A_p}{(E_p^2 - E^2 - i\gamma_p E)}. \quad (1)$$

where $n_b + ik_b$ represents the background complex refractive index of WSe_2 in the absence of excitons and was assumed to be equal to that of the bulk material[10] in the simulations. The index p stands for the type of exciton characterized by a resonance energy of E_p, with amplitude A_p and a phenomenological broadening parameter γ_p [equal to full width at half maximum (FWHM) of the lorentzian function]. The RC was then calculated using the transfer matrix formalism. To fully reproduce our experimental data, we introduced three additional oscillators in the dielectric function of the WSe_2 layers to account for the two observed exciton excited states and for the trion feature. The refractive indices of Si and the SiO_2 layers were obtained from Ref. 32. The results of this calculation for our different flakes are presented in Fig. 2(a) as dashed gray lines, together with the corresponding experimental data. We notice that the overall background shape of the reflectance contrast spectra has been reproduced quite well using transfer matrix method. Also, the Lorentz oscillator model has been able to reproduce the exciton lineshapes nicely. It is then tempting to express these results in the form of the absorption coefficient $\alpha(\lambda)$, defined as

$$\alpha(\lambda) = \frac{4\pi k}{\lambda}. \quad (2)$$

where k is the imaginary part of the refractive index. The calculated wavelength dependence of the absorption coefficient for the flakes are presented in Fig. 2(b).

The transition energies derived from the modelling of our data are presented in Fig. 3 as a function of the flake thickness. Both A and C-exciton energies decrease with increasing the number of layers, the effect being most pronounced for C. The energy of the B exciton appears to be only weakly dependent on the number of layers. Interestingly, the energy of both excited states A* and B* increases from 1 ML to 2 ML and then decreases for larger thicknesses. This peculiar evo-

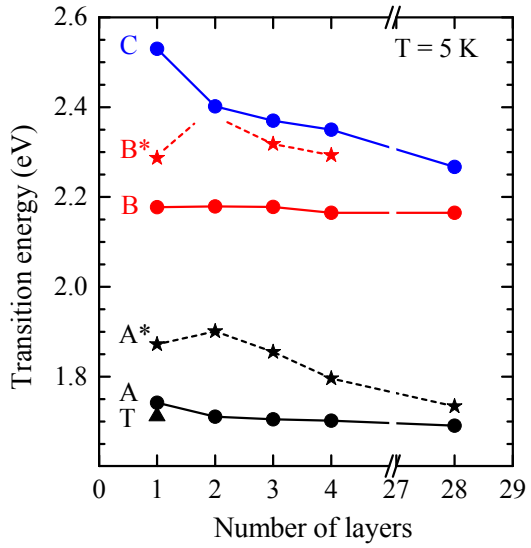

Figure 3: Transition energies of the features obtained after modeling the reflectance contrast spectra, for the excitons A, B and C, the excited state contributions of the excitons A* and B* and the trion T as a function of number of layers.

lution observed only for the exciton excited states is due to two competing effects. The first effect is the reduction of the exciton binding energy, possibly due to the change of the dielectric environment and of the dimensionality of the material from 2D- towards a more 3D system. The second effect is characteristic of TMDCs monolayers and arises from the nonlocal character of screening of the Coulomb interactions in such systems.[28,29,33] Indeed, exciton excited states in 1 ML WSe_2 strongly deviate from the hydrogenic Rydberg model,[28] verified for conventional 2D semiconductors. They were experimentally observed much closer in energy to the ground state than expected. This effect dominates in the case of the 1 ML flake but ceases to contribute when the number of layers is increased. When going from the monolayer to the thicker flakes, the excited state energy increases in a first step because the exciton structure recovers its Rydberg character but simultaneously, the exciton binding energy decreases when going towards the 3D limit. The latter effect dominates for stacks thicker than 3 ML and the excited state energy then decreases. This scenario has to be confirmed on theoretical grounds.

Assuming that the dominant contribution to the A* structure for the bulk comes from the n = 2 state of the exciton, we find an A exciton binding energy of ∼60 meV following the ideal Rydberg model for 3D case. This is in agreement with a previous report.[9] We notice that for 2 ML flake, the B* resonance merges with the C exciton peak and is omitted from the fitting procedure. For the bulk flake, the B* structure is too weak to be included in the analysis. From the RC fitting of the 1 ML thick flake, the trion (T) binding energy is estimated to be ∼30 meV which agrees quite well with a recently reported value.[15]

Ground state exciton: Temperature activated energy shift and broadening

To explore the properties of A exciton and T trions further, we performed μRC spectroscopy of the 1 ML thick flake as a function of temperature. In addition, we performed temperature dependent μRC measurements of A exciton in a 2 ML and a 20 nm thick bulk flake. Figures 4(a-c) show the evolution of the RC spectra around the A exciton peak as a function of temperature (5 K to 300 K) for 1 ML, 2 ML and 20 nm thick flake respectively, along with the calculated spectra. In the fitting procedure, we have also considered T for 1 ML and A* for the bulk flake. Commonly for the three studied films, the exciton resonance energies undergo a red shift with increasing temperature as shown in Fig. 4(d). This evolution, very typical for semiconductors, can be reproduced by the bandgap versus temperature relations, equally well when using the Varshni[34] or O'Donnell *et al.*[35] formulae. Varshni's relation is given by:

$$E_g(T) = E_0 - (\alpha T^2)/(T+\beta). \qquad (3)$$

where E_0 is the band gap at absolute zero, α and β are the fitting parameters related to the temperature-dependent dilatation of the lattice and Debye temperature respectively. Although, this relationship describes the evolution of band gap, it reproduces the exciton resonance energies equally well, which suggests the independence of exciton binding energy on temperature. The parameters which fit the data are given in Table 1. We no-

Table 1: Fitting parameters as obtained from fitting of temperature dependence of the ground state exciton resonance energies and lineshape broadenings for 1 ML, 2 ML and bulk WSe_2 flakes

Parameter	1 ML	2 ML	Bulk
Using Equation 3			
E_0 (eV)	1.744	1.717	1.692
$\alpha(\times 10^{-4} eVK^{-1})$	4.24	3.58	3.44
β (K)	170	170	170
Using Equation 4			
E_0 (eV)	1.742	1.716	1.691
$\langle\hbar\omega\rangle$ (meV)	15	15	15
S	2.06	1.75	1.67
Using Equation 5			
γ_0 (meV)	15	34	26
γ' (meV)	78	75	105

tice that the parameter α shows a reduction as the thickness of the flake is increased from 1 ML to 2 ML and bulk. Notably, there is a fundamental change in the crystal lattice when the thickness is increased from 1 ML thickness onwards. However, the β parameter is $\sim$170 K for all the three kinds of flakes, and it was fixed to this value during the fitting. The effective Debye temperature seems therefore to be independent of the film thickness. Our estimation of β parameter of WSe_2 is in agreement with a previous report of Hu et al. where a value of $\beta = 160$ K was found from the photoconductivity measurements on bulk crystals.[36] The relation provided by O'Donnell et al. describes the band gap dependence on temperature in terms of average phonon energy $\langle\hbar\omega\rangle$, as the following

$$E_g(T) = E_0 - S\langle\hbar\omega\rangle[\coth(\langle\hbar\omega\rangle/2kT) - 1]. \quad (4)$$

where S is a coupling constant. The parameters obtained for the best fit are given in Table 1. Similar to β parameter, $\langle\hbar\omega\rangle$ stays nearly the same $\sim$15 meV, and its value was fixed during fitting. The S parameter shows a gradual decrease from the monolayer to the bulk. Both relations produce seemingly indistinguishable fits to the data, and the curves corresponding to Eq. 4 are shown in Fig. 4(d).

Figure 4(e) shows the temperature dependence of linewidth broadenings (γ_p in Eq. 1) obtained

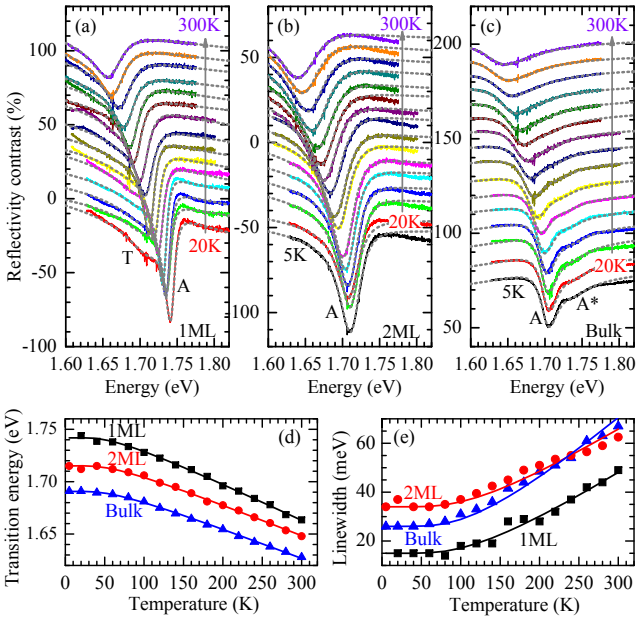

Figure 4: (a-c) show the reflectance contrast spectra of the 1 ML, 2 ML and bulk flakes as a function of temperature, in an energy region around the lowest energy exciton peak. The dashed lines represent the corresponding lineshape fittings to the spectra. The spectra were measured at 5 K (not available for 1 ML in this set of measurements), 20 K and then upto 300 K in steps of 20 K. In all the cases, the spectra have been shifted along the **y**-axis for clarity. (d) Filled squares, circles and triangles show the variation of the exciton band gap of 1 ML, 2 ML and the bulk flake respectively, as a function of temperature. The grey lines are the fits to the data using Eq. 4.

from the fits in Figs. 4(a-c). In semiconductors, the temperature dependence of the width of the n = 1 ground state exciton has the form[37]

$$\gamma(T) = \gamma_0 + \sigma T + \gamma' \frac{1}{e^{\hbar\omega/kT} - 1}. \quad (5)$$

where γ_0 is the broadening at 0 K, the term linear in T depicts the interaction of excitons with acoustic phonons and the last term arises from interaction with LO (longitudinal optical) phonons. The former is neglected being negligibly small compared to the latter, which is proportional to the Bose function for LO-phonon occupation. $\hbar\omega$ is the LO-phonon energy and is taken to be equal to 31.25 meV (250 cm^{-1}) for WSe_2.[7] The fits to the data are shown as solid lines in Fig. 4(e) and

the fitting parameters are shown in Table 1. We notice that γ_0, which depends on the film quality, is different for the three films studied. However, γ' is similar for 1 ML and 2 ML flakes, whereas it is larger for the bulk film. It can be understood as follows. For 1 ML and 2 ML films, the binding energy of the exciton is much larger than the LO phonon energy, therefore the probability of scattering of the ground state exciton to its excited bound and continuum states through the LO-phonons is negligible.[37] In such a case, the scattering of the exciton assisted by an annihilation of LO-phonons is mostly permissible within the n = 1 state, to higher in energy excitonic states with larger center-of mass momentum. However, for the bulk case, the exciton binding energy is comparable to that of LO-phonon energy. Therefore, the ground state exciton has a significant probability to scatter to the energetically accessible excited exciton states through annihilation of an LO-phonon. Such additional contributions give rise to an increase in broadening in the bulk flake as compared to the 1 and 2 ML flakes at elevated temperatures, in turn increasing the slope of the γ(T) curve.

Excitons and charged excitons in 1 ML flake

The monolayers of SC-TMDCs are commonly accepted to be the direct band gap semiconductors and their optical response in the vicinity of the band edge is understood in terms of the associated excitonic resonances (free-, charged- and localized/bound excitons). At low temperatures and in the presence of impurities and/or free carries, the localized/bound and/or charged exciton states (trions) usually dominate the PL response of direct gap semiconductors whereas the free exciton emission is rather weakly pronounced. This picture can also be applied to account for low temperature spectra of our WSe_2 monolayer, as shown in the bottom traces in Fig. 5(a). These spectra consist of up to four emission peaks which, in line with the previous studies, can be attributed to the neutral exciton (A), charged exciton (T, trion) and two localized/bound excitons (L1 and L2).[15] The observed evolution of the μPL spectra with temperature is, however, intriguing. To begin with, when the temperature is raised, the L1 and L2 peaks disappear from the spectra (at $\sim$40 K) initially whereas the higher energy trion emission survives up to considerable higher temperatures (up to $\sim$200 K). The opposite would be expected when naively assuming that lower in energy excitonic complexes should have higher dissociation/activation energies. This assumption may not, however, apply to TMDCs' monolayers for which the T complexes have been speculated to exhibit higher dissociation energies than the impurity-bound excitons,[16] in overall agreement with our observation. Regardless of the apparent dissociation energies, the PL dynamics is another relevant parameter which has to be taken account when discussing the PL changes with temperature. Time resolved PL studies of WSe_2 monolayers show that A-exciton emission decays rather fast (few picoseconds decay time) whereas the decay time of the subsequent lower in energy PL peaks progressively increases up to $\sim$100 ps for the L2 peak.[15] The temperature-activated population of higher energy states, which presumably give rise to the emission more effectively could also qualitatively account for the observed temperature-activated redistribution of the PL intensity among different emission peaks.

This redistribution itself can be qualitatively understood but the observed rise of the integrated PL intensity with temperature (inset to Fig. 5(a)) is a veritable puzzle. Typically in semiconductors, a quenching of the PL intensity is observed with increasing temperature. The observed rise of the PL yield (integrated intensity) is particularly striking because it appears at relatively higher temperatures where all the emission appears to arise due to recombination of free excitons. We do not have a solid explanation for this effect but cannot restrain from speculating on its possible origin. We put forward an hypothesis where we speculate an existence of certain dark, optically inactive states in the WSe_2 monolayer, below the ground state A exciton. Those dark states could be associated with the excitons indirect in k-space, which is however in contradiction with a general belief that the WSe_2 monolayer is a direct gap semiconductor,[13] (though the consensus in this matter may not have been reached so far[14]). Optionally one could spec-

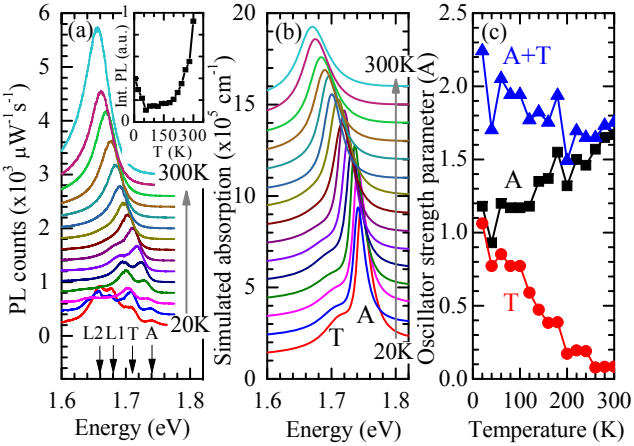

Figure 5: (a) and (b) show the PL and absorption spectra (derived from reflectance) for 1 ML thick flake as a function of temperature, in an energy region around the lowest energy exciton peak. The arrows in (a) represent the energy positions of the indicated spectral features at 20K and the inset shows the integrated PL intensity as a function of temperature. (c) Squares and circles show the temperature dependence of the oscillator strength parameter of the exciton, A and the trion, T. Triangles show the total oscillator strength parameter.

ulate about other dark excitonic states, similar to the exchange-split dark excitons in conventional semiconductors,[38] in case of the specific alignment of the signs of the spin-orbit splitting in the conduction and valence bands of the WSe_2 monolayer.[39] The existence of such states could also qualitatively account for a double exponential decay of the A-emission reported recently from time resolved experiments.[15] Nonetheless, firm conclusions about the fine structure of the fundamental exciton in WSe_2 monolayer require further experiments and theoretical studies.

The appearance of charged excitons in SC-TMDCs has been largely discussed in literature,[6,19] though their identification has been so far based on the PL spectroscopy only. Most convincing with this respect are the PL experiments carried out as a function of the gate voltage (carrier concentration),[6] nevertheless the distinction between the bound/localized and (free) trion states as observed in low temperature PL is rather a subtle issue. Vast studies of conventional two dimensional structures (e.g. CdTe[17] and GaAs[20]) show that charged excitons are characterized by the significant oscillator strength and should be also visible in absorption type spectra, whereas bound/localized excitons may be predominant in the PL spectra. With the results shown in Fig. 5, obtained for one of our 1 ML layer flakes, we identified the trion peak (T) on the low energy side of the A exciton in the low temperature PL [Fig. 5(a)] and in the absorption type spectra [Fig. 5(b)] as well. Observation of trions in absorption spectra is further confirmed by spectral evolution with temperature. A characteristic transfer of the oscillator strength from the trion to neutral exciton is observed upon increasing the temperature. This effect is analogous to what has been largely discussed in the context of optical studies of (weakly doped) CdTe and GaAs quantum wells.[20–24] Generally speaking, the loss and gain of the oscillator strength of charged and neutral exciton with temperature, respectively, is due to the thermal redistribution of free carriers from Fermi-Dirac statistics at low temperature towards Boltzmann distribution at higher temperatures. The increase of temperature opens the k-space around the band edge for the efficient formation of the neutral exciton which leads to its increased oscillator strength. On the other hand, the weakening of the oscillator strength of charged excitons associated with carriers with higher k-wave vectors explains the progressive disappearance of the trion absorption with temperature. Quantitative analysis of the transfer of the oscillator strength from trion to neutral exciton remains to be done in future, on samples with the controlled carrier concentration. Interestingly, the evolution of the optical response with carrier concentration may scale very differently in SC-TMDCs monolayers than in conventional semiconductors, due specific form of Coulomb interaction and non-Rydberg character of excitons in the former systems.[28,29]

Conclusions

In conclusion, we have studied the excitonic band structure of layered WSe_2 semiconductor as a function of layer thickness and temperature. We presented a comprehensive lineshape analysis of the RC spectra, and deduced the exciton transition energies. The exciton transitions taking place

at the K-point and M-point of the Brillouin zone were observed in the spectral energy range of ∼1.6 - 2.7 eV. The parameters dictating the temperature activated energy shift and broadening of the fundamental absorption resonance have been determined for 1 ML, 2 ML and bulk WSe_2 samples. The formation of a charged exciton (trion) in WSe_2 monolayer has been traced with absorption type experiments and the transfer of the oscillator strength from the trion to exciton has been observed upon increasing the temperature. The observation of a striking rise of the PL yield with temperature in a monolayer WSe_2 opens up a scope for further theoretical and experimental investigations of this system.

Methods

The monolayer (ML) and a few layer (FL) WSe_2 flakes were obtained on Si/(100 nm)SiO_2 substrate using mechanical exfoliation techniques.[11] The flakes of interest were first identified by visual inspection under a microscope. A transfer matrix based calculation was performed to predict the color of the flake as a function of its thickness.[41] The observed color of the flake was then compared with the theoretically predicted one to roughly estimate the number of layers in the flakes. For performing μPL measurements, the 632.8 nm radiation from He-Ne laser was focused on the flake using a 50x long working distance objective. The sample was mounted on the cold finger of a continuous flow liquid helium cryostat, at a temperature of ∼5 K. The spot diameter was ∼2 μm and the light power focused on the sample was 5 μW for 1 ML, 50 μW for 2 ML and 250 μW for the thicker layers. The PL emission from the sample was dispersed using a 0.5 m focal length monochromator and detected using a liquid nitrogen cooled Si charge coupled device camera. The setup for performing μPLE was similar to the one used for μPL, except that a tunable Ti-sapphire laser with wavelength ranging from 700 nm to 800 nm was used for excitation. The intensity of the emission at a certain detection wavelength for each flake was monitored as a function of the excitation wavelength to record the PLE spectrum. For performing the μRC measurements, the light from a 100 W tungsten halogen lamp was focused on a pinhole of 150 μm diameter. The light was then collimated and focused (spot size ∼4 μm) on the sample. The reflected light was detected using a setup similar to the one used for performing μPL. If $\mathscr{R}(\lambda)$ and $\mathscr{R}_0(\lambda)$ are the reflectance spectra of the WSe_2 flake and the Si/SiO_2 substrate respectively, as a function of the wavelength (λ), then the percentage reflectance contrast spectrum is defined as follows:

$$\mathscr{C}(\lambda) = \frac{\mathscr{R}(\lambda) - \mathscr{R}_0(\lambda)}{\mathscr{R}(\lambda) + \mathscr{R}_0(\lambda)}. \quad (6)$$

The measurements were performed at temperatures ranging from 5 K to 300 K. It must be mentioned that the RC spectrum shown for 1 ML flake in Fig. 2 was measured after approximately 1 month than the spectra shown in Fig. 4(a). We notice that the overall spectral intensity of the RC exciton features was reduced to about half when the sample was around 1 month old due to the effects of sample aging. In addition, the oscillator strength of the trion peak showed an increase after 1 month, which is possibly due the spontaneous doping of the sample in atmosphere. However, the energy positions of the spectral signatures did not show any noticeable shift.

Acknowledgement We thank Piotr Kossacki for useful discussions, Ivan Breslavetz for technical support and Sandip Ghosh for valuable suggestions during building of the μRC setup. We acknowledge the support from the EC Graphene Flagship project (No. 604391) and the European Research Council (MOMB project No. 320590).

References

1. Mak, K.; Lee, C.; Hone, J.; Shan, J.; Heinz, T. F. Atomically Thin MoS_2: A New Direct-Gap Semiconductor. *Phys. Rev. Lett.* **2010**, *105*, 136805.

2. Wang, Q. H.; Kalantar-Zadeh, K.; Kis, A.; Coleman, J. N.; Strano M. S. Electronics and Optoelectronics of Two-Dimensional Transition Metal Dichalcogenides. *Nat. Nanotechnol.* **2012**, *7*, 699-712.

3. Eda, G.; Maier, S. A. Two-Dimensional Crystals: Managing Light for Optoelectronics. *ACS Nano* **2013**, *7*, 5660-5665.

4. Butler, S. Z.; Hollen, S. M.; Cao, L.; Cui, Y.; Gupta, J. A.; Gutiérrez, H. R.; Heinz, T. F.; Hong, S. S.; Huang, J.; Ismach, A. F. Progress, Challenges, and Opportunities in Two-Dimensional Materials Beyond Graphene *ACS Nano* **2013**, *7(4)* 2898âĂŞ 2926.

5. Xiao, D.; Liu, G. B.; Feng, W.; Xu, X.; Yao, W. Coupled Spin and Valley Physics in Monolayers of MoS_2 and Other Group-VI Dichalcogenides. *Phys. Rev. Lett.* **2012**, *108*, 196802.

6. Jones, A. M.; Yu, H.; Ghimire, N. J.; Wu, S.; Aivazian, G.; Ross, J. S.; Zhao, B.; Yan, J.; Mandrus D. G.; Xiao, D.; Yao, W.; Xu, X. Optical Generation of Excitonic Valley Coherence in Monolayer WSe_2. *Nat. Nanotechnol.* **2013**, *8*, 634-638.

7. Tonndorf, P.; Schmidt, R.; Böttger, P.; Zhang, X., Börner, J.; Liebig, A.; Albrecht, M.; Kloc, C.; Gordan, O.; Zahn, D. R. T.; Michaelis de Vasconcellos, S.; Bratschitsch, R. Photoluminescence Emission and Raman Response of Monolayer MoS_2, $MoSe_2$, and WSe_2. *Opt. Express* **2013**, *21*, 4908-4916.

8. Wilson, J. A.; Yoffe, A. D. The Transition Metal Dichalcogenides Discussion and Interpretation of the Observed Optical, Electrical and Structural Properties. *Adv. Phys.* **1969**, *18(73)*, 193-335.

9. Beal, A. R.; Knights, J. C.; Liang, W. Y. Transmission Spectra of Some Transition Metal Dichalcogenides: II. Group VIA: Trigonal Prismatic Coordination. *J. Phys. C: Solid State Phys.* **1972**, *5*, 3540-3551.

10. Beal, A. R.; Liang, W. Y.; Hughes, H. P. Kramers-Krönig analysis of the reflectivity spectra of 3R-WSe_2. **1976**, *9*, 2449-2457.

11. Novoselov, K. S.; Jiang, D.; Schedin, F.; Booth, T. J.; Khotkevich, V. V.; Morozov, S. V.; Geim, A. K. Two-Dimensional Atomic Crystals. *Proc. Natl. Acad. Sci. U.S.A.* **2005**, *102*, 10451-10453.

12. Yun, W. S.; Han, S. W.; Hong, S. C.; Kim, I. G.; Lee, J. D. Thickness and Strain Effects on Electronic Structures of Transition Metal Dichalcogenides: 2H-MX_2 Semiconductors (M = Mo, W; X = S, Se, Te). *Phys. Rev. B* **2012**, *85*, 033305.

13. Zhao, W.; Ghorannevis, Z.; Chu, L.; Toh, M;, Kloc, C.; Tan, P.-H.; Eda, G. Evolution of Electronic Structure of Atomically Thin Sheets of WS2 and WSe2. *ACS nano* **2013**, *7*, 791-797.

14. Ramasubramaniam, A. Large Excitonic Effects in Monolayers of Molybdenum and Tungsten Dichalcogenides. *Phys. Rev. B* **2012**, *86*, 115409.

15. Wang, G.; Bouet, L.; Lagarde, D.; Vidal, M.; Balocchi, A.; Amand, T.; Marie, X.; Urbaszek, B. Valley Dynamics Probed Through Charged and Neutral Exciton Emission in Monolayer WSe_2. *Phys. Rev. B* **2014**, *90*, 075413.

16. Aleiner, I.; Fal'ko, V.; Glanchev, B. Three-particle Complexes in Two-Dimensional Semiconductors. *Preprint at arXiv:1408.3981 [cond-mat.mes-hall]* **2014**.

17. Kheng, K.; Cox, R. T.; d'Aubigné, Y. M.; Bassani, F.; Saminadayar, K.; Tatarenko, S. Observation of Negatively Charged Excitons X^- in Semiconductor Quantum Wells. *Phys. Rev. Lett.* **1993**, *71*, 1752-1755.

18. Buhmann, H.; Mansouri, L; Wang, J.; Beton, P. H.; Mori, N.; Eaves, L.; Henini, M.; Potemski, M. Electron-concentration-dependent Quantum-well Luminescence: Evidence for a Negatively Charged Exciton. *Phys. Rev. B* **1995**, *51*, 7969-7972.

19. Mak, K. F.; He, K.; Lee, C.; Lee, G. H.; Hone, J.; Heinz, T. F.; Shan, J. Tighly Bound Trions in Monolayer MoS_2. *Nat. Mater.* **2013**, *12*, 207-211.

20. Finkelstein, G.; Shtrikman, H.; Bar-Joseph, I. Optical Spectroscopy of a Two-Dimensional Electron Gas Near the Metal-Insulator Transition. *Phys. Rev. Lett.* **1995**, *74*, 976-979.

21. Ciulin, V.; Kossacki, P.; Haacke, S.; Ganière, J.-D.; Deveaud, B.; Esser, A. Radiative Behavior of Negatively Charged Excitons in CdTe-Based Quantum Wells: A Spectral and Temporal Analysis. *Phys. Rev. B* **2000**, *62*, R16310-R16313.

22. Kossacki, P. Optical Studies of Charged Excitons in II-VI Semiconductor Quantum Wells. *J. Phys: Condens. Matter* **2003**, *15*, R471-R493.

23. Suris, R. A.; Kochereschko, V. P.; Astakhov, G. V.; Yakovlev, D. R.; Ossau, W.; Nürnberger, J.; Faschinger, W.; Landwehr, G.; Wojtowicz, T.; Karczewski, G.; Kossut, J. Excitons and Trions Modified by Interaction with a Two-Dimensional Electron Gas. *Phys. Stat. Sol. (b)* **2001**, *227*, 343-352.

24. Esser, A.; Zimmermann, R.; Runge, E. Theory of Trion Spectra in Semiconductor Nanostructures. *Phys. Stat. Sol. (b)* **2001**, *227*, 317-330.

25. Zhao, W.; Ghorannevis, Z.; Amara, K. K.; Pang, J. R.; Toh, M.; Zhang, X.; Kloc, C.; Tan, P. H.; Eda, G. Lattice Dynamics in Mono- and Few-Layer Sheets of WS_2 and WSe_2. *Nanoscale* **2013**, *5*, 9677-9683.

26. del Corro, E.; Terrones, H.; Elias, A.; Fantini, C.; Feng, S.; Nguyen, M. A.; Mallouk, T. E.; Terrones, M.; Pimenta, M. A. Excited Excitonic States in 1L, 2L, 3L and Bulk WSe_2 Observed by Resonant Raman Spectroscopy. *ACS Nano* **2014**, *8*, 9629-9635.

27. Kormányos, A.; Burkard, G.; Gmitra, M.; Fabian, J.; ZÁşlyomi, V.; Drummond, N. D.; Fal'ko, V. $\mathbf{k}\cdot\mathbf{p}$ Theory for Two-Dimensional Transition Metal Dichalcogenide Semiconductors. *Preprint at arXiv:1410.6666 [cond-mat.mes-hall]* **2014**.

28. He, K.; Kumar, N.; Zhao, L.; Wang, Z.; Mak, K. F.; Zhao, H.; Shan, J. Tightly Bound Excitons in Monolayer WSe_2. *Phys. Rev. Lett.* **2014**, *113*, 026803.

29. Chernikov, A.; Berkelbach, T. C.; Hill, H. M.; Rigosi, A.; Li, Y.; Aslan, O. B.; Reichman, D. R.; Hybertsen, M. S.; Heinz, T. F. Exciton Binding Energy and Nonhydrogenic Rydberg Series in Monolayer WS_2. *Phys. Rev. Lett.* **2014**, *113*, 076802.

30. Zhao, W.; Ribeiro, R. M.; Toh, M.; Carvalho, A.; Kloc, C.; Neto, A. H. C.; Eda, G. Origin of Indirect Optical Transitions in Few-Layer MoS_2, WS_2, and WSe_2. *Nano Lett.* **2013**, *13*, 5627âĹŠ5634.

31. Arora, A.; Mandal, A.; Chakrabarti, S.; Ghosh, S. Magneto-Optical Kerr Effect Spectroscopy Based Study of Landé g-Factor for Holes in GaAs/AlGaAs Single Quantum Wells Under Low Magnetic Fields. *J. Appl. Phys.* **2013**, *113*, 213505.

32. Palik, E. D. Handbook of Optical Constants of Solids, Vol. 1 *Academic Press, London* **1998**.

33. Qiu, D. Y.; Jornada, F. H. D.; Louie, S. G. Optical Spectrum of MoS_2: Many-Body Effects and Diversity of Exciton States. *Phys. Rev. Lett.* **2013**, *111*, 216805.

34. Varshni, Y. P. Temperature Dependence of the Energy Gap in Semiconductors. *Physica* **1967**, *34*, 149-154.

35. O'Donnell, K. P.; Chen, X. Temperature Dependence of Semiconductor Band Gaps. *Appl. Phys. Lett.* **1991**, *58*, 2924-2926.

36. Hu, S. Y.; Lee Y. C.; Shen, J. L.; Chen, K. W.; Huang, Y. S. Urbach Tail in the Absorption Spectra of 2H-WSe_2 Layered Crystals. *Phys. Stat. Sol. (a)* **2007**, *204*, 2389-2395.

37. Rudin, S.; Reinecke, T. L.; Segall, B. Temperature-Dependent Exciton Linewidths in Semiconductors. *Phys. Rev. B* **1990**, *42*, 11218-11231.

38. Chen, Y.; Gil, B.; Lefebvre, P.; Mathieu, H. Exchange Effects on Excitons in Quantum Wells. *Phys. Rev. B* **1988**, *37*, 6429-6432.

39. Kośmider, K.; González, J. W.; Fernández-Rossier, J. Large Spin Splitting in the Conduction Band of Transition Metal Dichalcogenide Monolayers. *Phys. Rev. B* **2013**, *88*, 245436.

40. Klingshirn, C. Semiconductor Optics, 2nd Edition. *Springer-Verlag, Berlin Heidelberg* **2005**.

41. Hecht, E. Optics, 4th Edition. *Addison-Wesley, New York* **2002**.